



ARHGAP17 Inhibits Hepatocellular Carcinoma Progression by Inactivation of Wnt/ β -Catenin Signaling Pathway

Sirui Fan^{1,2} · Hongqing Zhao³ · Cheng Li⁴ · Xing Chen² · Mingjie Sun² · Fengyang Chen² · Chao Long² · Yinghui Zhou² · Boyuan Nan² · Hao Zhao² · Wei Zhang²

Received: 28 May 2023 / Accepted: 27 April 2024

© The Author(s), under exclusive licence to Springer Science+Business Media, LLC, part of Springer Nature 2024

Abstract

As a member of Rho GAPs family, Rho GTPase-Activating Protein 17 (ARHGAP17) regulates cytoskeletal recombination, cell polarity, cell proliferation and cell migration. ARHGAP17 is identified as a tumor suppressor in numerous cancer types. Current study intends to examine ARHGAP17 expression and its possible influence on the progression of hepatocellular carcinoma (HCC). ARHGAP17 expression in HCC cells was verified by RT-PCR and western blot. The proliferation and invasion of HCC cells were evaluated by CCK8 assay and transwell assay, respectively. The mRNA expression of ARHGAP17, PCNA, E-cadherin, N-cadherin, β -catenin, GSK-3 β , Axin1, and APC were detected by RT-PCR. The protein expression of ARHGAP17, PCNA, E-cadherin, N-cadherin, β -catenin, p- β -catenin, GSK-3 β , p-GSK-3 β , Axin1, and APC were detected by western blot. ARHGAP17 staining was evaluated by immunohistochemistry and immunofluorescence. ARHGAP17 expression decreased significantly in HCC tumors and HCC cells after EMT. In response to overexpression of ARHGAP17, the capacities of HCC cell proliferation and invasion were reduced significantly, which were also confirmed by tumorigenesis experiments *in vivo*. With overexpression of ARHGAP17 in HCC cells, the p-GSK3 β /GSK3 β decreased, while the p- β -catenin/ β -catenin, Axin1 and APC increased. In conclusion, ARHGAP17 inhibits HCC progression by inactivating the Wnt/ β -catenin signaling pathway.

✉ Wei Zhang
zhang_wei_1980@163.com

¹ Graduate Training Base, General Hospital of Northern Theater Command of Jinzhou Medical University, Shenyang 110016, Liaoning, China

² Department of Hepatobiliary Surgery, General Hospital of Northern Theater Command, No. 83 Wenhua Road, Shenyang 110016, Liaoning, China

³ Graduate School, Jinzhou Medical University, Jinzhou 121000, Liaoning, China

⁴ Department of Immunology, The College of Basic Medical Sciences, China Medical University, Shenyang 110122, Liaoning, China

Keywords ARHGAP17 · Hepatocellular carcinoma · EMT · Wnt/ β -catenin

Introduction

The global prevalence of chronic hepatitis C virus (HCV) infection was estimated to be 71 million people by the World Health Organization (WHO) in 2020 (Rabaan et al. 2020). HCV infection is a common risk factor for hepatocellular carcinoma (HCC) (McGlynn et al. 2021). As acknowledged, HCC onset consists of multiple processes including numerous risk factors, however, it always presents in people with chronic liver diseases and cirrhosis (Ghouri et al. 2017). Despite the achievements in a range of treatment methods, the prognosis for patients with HCC remains poor owing to the metastasis and recurrence after surgical resection (Forner et al. 2018). It is urgent to further elucidate the underlying molecular mechanisms of HCC progression and develop novel therapeutic approaches.

Rho GTPases serve as molecular switches in diverse fundamental cellular processes, including cell cycle, cytoskeletal organization, and cell migration, etc. (Jaffe and Hall 2005). Rho GTPase activating proteins (RhoGAPs) promote the transition of RhoGTPases from an active GTP-bound state to an inactive GDP-bound state (Braun and Olayioye 2015). Rho GTPase Activating Protein 17 (ARHGAP17, Rich1, Nadrin) is a member of RhoGAPs (Richnau and Aspenström 2001). ARHGAP17 exerts numerous functions, for instance, ARHGAP17 negatively regulate the epithelial cell cycle, proliferation, and focal adhesion by CDC42/RAC1-PAK1-ERK1/2 signaling pathway and F-actin dynamics (Zhang et al. 2015), ARHGAP17 inhibits the apoptosis of human PDL fibroblasts induced by pathological periodic strain by inactivating Rac1/Cdc42 (Wang et al. 2020a, b), ARHGAP17 regulates the spatiotemporal activity of Cdc42 at invadopodia (Kreider-Letterman et al. 2023).

In recent years, ARHGAP17 has been reported as a tumor suppressor of malignant tumors, e.g., ARHGAP17 up-regulates the expressions of p21 and p27 by inhibiting the PI3K/AKT signaling pathway, thereby inhibiting the malignant proliferation of cervical cancer cells (Guo et al. 2019), ARHGAP17 inhibits tumor progression and metastasis of colon cancer by Wnt/ β -catenin signaling pathway (Pan et al. 2018), ARHGAP17 suppresses breast cancer stem cell traits by activating kinases cascade of Hippo signaling (Tian et al. 2022). However, the exact role of ARHGAP17 in HCC and its related molecular mechanism remains to be studied.

Materials and Methods

Tissue Samples

At first, 12 cases of human HCC tissues and 11 cases of para-cancer tissues were collected from patients who were treated in the General Hospital of Northern Theater Command of PLA. Tissues were immediately stored after extraction. Current study was approved by the Ethics Committee of the General Hospital of Northern Theater Command of PLA.

Cell Culture

Human HCC cell lines (Bel-7405 and HuH7) were donated by the Immunology Laboratory of China Medical University. All of the cells were added to DMEM (Cat # SH30022.01, Hyclone) containing 10% of fetal bovine serum (Cat # 10099141C, Gibco) and 1% of penicillin–streptomycin (Cat # Solarbio, P1400) for routine culture. The third passage of cells was adopted in the experiment.

TGF- β (5 ng/ml) was used to induce epithelial-mesenchymal transformation (EMT) of HCC cells according to previous reports (Shao et al. 2015; Malfettone et al. 2017).

Lentiviral Construction

Human ARHGAP17 full-length cDNA was constructed into the pLV (Exp)-EGFP: T2A: Puro-EF1A to construct ARHGAP17 vector (2 μ g, Genechem, Shanghai, China) and induce ARHGAP17 overexpression. Cells (3×10^5 cells/well) transfected with pLV (Exp)-EGFP: T2A: Puro-EF1A vector (Genechem) were used as negative control (empty vector, 2 μ g). Cell transfection was conducted by Lipofectamine® 2000 (Thermo Fisher Scientific, Wilmington, DE, USA) for 48 h at 37 °C. Subsequently, cells were collected for the following experimentations.

ARHGAP17 (GeneBank accession no. NM_000016.10) was introduced into MerMade192E (Bioautomation, USA) to complete primer synthesis. Then, 2 h of ammoniolysis was carried out by a gas phase cleavage device, after addition of 200 μ l of acetonitrile, pump drying and cleaning were performed 3 times under negative pressure. Finally, DNA denaturation, 2 h of electrophoresis, foam and primer recovery were carried out.

After reaching a confluence of ~70–80%, 293 T cells were transfected with NC and ARHGAP17 lentiviral vectors. After 48 h, the viruses were harvested and concentrated, and their titers were detected. For lentiviral infection, Bel-7405 and HuH7 cells (3×10^5 cells/well) were planted in a 6-well plate, when cells had grown to a confluence of ~90%, the experimental lentivirus (2nd generation, 8 μ g, plvx, psPAX2, psMD2.G=4: 3: 1) at a multiplicity of infection (MOI) of 20 in the presence of polybrene was used to transfect the cells at 37 °C for 72 h. Following infection, the transfection medium was discarded and replaced by selective medium including 2 μ g/ml puromycin (Sigma-Aldrich; Merck KGaA) for 9 days, then maintained in medium including 1 μ g/ml puromycin (Sigma-Aldrich). Afterwards, the third passage of stable clones was collected in the following experiments. The transfection efficiency was evaluated using reverse transcription-quantitative PCR (RT-qPCR) and western blot analysis.

CCK8 Assay

Cells were inoculated into a 96-well plate after trypsin digestion (Cat# KR11825200056, Gibco), then underwent 8 h of adherence and growth. Next, each

well was added with 10 μ l of CCK8 reagent (Cat#HY-K0301, MCE) and incubated at 37°C for 4 h. After that, the absorbance at 12, 24, 36, and 48 h was measured at 450 nm using a multimode microplate reader (Biotek Synergy2, USA).

Cell Invasion Assay

An invasion detection was performed on the transwells (8 μ m well; Corning, New York, NY, USA) coated with matrigel (1 mg/ml; Corning). Cells were cultured in a 60 mm diameter petri dish for 24 h, the upper chamber was added with cells from serum-free DMEM (5×10^4 cells/well), while the lower chamber with DMEM containing 10% FBS (5×10^4 cells/well). After 24 h of incubation at 37 °C with 5% CO₂, the unigrated cells were completely removed with cotton swabs, while the remaining cells were fixed, stained with crystal violet, and placed under an optical microscope (Leica) for observation and counting. Cells were treated with Mitomycin C (12.5 ng/ml, Sigma-Aldrich, St. Louis, MO, USA) for 3 h before being added to the upper chamber to inhibit cell proliferation (Sribenja et al. 2013).

Tumor Growth

Animal experimentations were reviewed and approved by the Ethics Committee of the General Hospital of the Northern Theater Command of the PLA. The male BALB/C nude mice (SPF Biotechnology, Beijing, China) aged 8 weeks were randomized into three groups ($n=5$). Each mouse was inoculated with 5×10^6 cells at the right axilla to induce an ectopic tumor. The tumor nodule volume was measured once every 6 days. The tumor volume (V) was calculated as $V=(a \times b^2)/2$, where “ a ” and “ b ” represented the long and short axes of the tumor nodule, respectively. The tumor nodules were excised and weighed at day 40 after inoculation.

RT-PCR

Total RNA was extracted with Trizol (Cat # 15596026, Thermo Fisher, Waltham, MA, USA), its purity and concentration were determined by a UV spectrophotometer (NanoDrop 2000, Thermo Fisher). A 20 μ l reverse transcription system was prepared according to the instructions for use of FastKing gDNA Dispelling RT SuperMix (Cat # KR118, TianGen, China), and stored at 4 °C after 15 min of incubation at 42 °C and 3 min at 95 °C in a T100 thermal cycler (Bio-RAD, Hercules, CA, USA). Then cDNA was subjected to RT-PCR by Top Green qPCR SuperMix, on CFX Connect real-time system (BIO-RAD, Hercules, CA, USA). The reaction was performed as follows: 94 °C for 30 s, followed by 45 cycles of 95 °C for 5 s, 56 °C for 15 s, 72 °C for 10 s. For each well, CT value was recorded, gene expression was normalized to GAPDH by the $2^{-\Delta\Delta C_t}$ method. The primer sequences are shown in Table 1.

Table 1 Primers used for real-time polymerase chain reaction

Gene	Primer sequences
E-cadherin	Forward 5'-TTTGAAGATTGCACCGGTGCG-3' Reverse 5'-CAGCGTGACTTTGGTGAAAA-3'
N-cadherin	Forward 5'-TTTGTATGGAGGTCTCCTAACACC-3' Reverse 5'-ACGTTTAAACACGTTGGAAATGTG-3'
ARHGAP17	Forward 5'-CCTCTGTACGGCATAGCTGAG-3' Reverse 5'-TGAGGATTTGTGAGCTTGGTTC-3'
β -catenin	Forward 5'-AAAGCGGCTGTTAGTCACTGG-3' Reverse 5'-CGAGTCATTGCATACTGTCCAT-3'
GSK3 β	Forward 5'-GGCAGCATGAAAGTTAGCAGA-3' Reverse 5'-GGCGACCAGTTCTCCTGAATC-3'
AXIN1	Forward 5'-GGTTTCCCTTGGACCTCG-3' Reverse 5'-CCGTCGAAGTCTCACCTTTAATG-3'
APC	Forward 5'-GCTGCACAACATCGTCTTCTC-3' Reverse 5'-ACGGCGGTACTCCTCATCA-3'
GAPDH	Forward 5'-AAAATCAAGTGGGGCGATGCT-3' Reverse 5'-TGTTTCACACCCATGACGAAC-3'
Mouse PCNA	Forward 5'-ATGTTTGAGGCACGCCTGATCCAG-3' Reverse 5'-CTAAGATGCTTCTCCTCACTTCAATC-3'
Mouse GAPDH	Forward 5'-CCTGCCAAGTATGATGACAT-3' Reverse 5'-GTTGCTGTAGCCGTATTCA-3'

Western Blot

The cell precipitate was collected and cleaned by PBS three times prior to the extraction of the total protein. In short, the protease inhibitor (Cat#36978, Thermo Fisher) and phosphatase inhibitor (Cat#A32957, Thermo Fisher) were added to the RIPA lysis fluid (Cat#89901, Thermo Fisher) at the volume ratio of 100:1:1, for homogenization on ice. The protein concentration was determined by a UV spectrophotometer. A total protein of 40 μ g was separated by SDS-PAGE, transferred to a PVDF membrane (Cat#IPVH00010, Millipore, Merck). Afterwards, the PVDF membrane was blocked with 5% skim milk at room temperature for 1 h, followed by incubation overnight with anti-ARHGAP17 (Cat#ab74454, 1:1000, Abcam), anti-E-cadherin (Cat#ab1416, 1:1000, Abcam), anti-N-cadherin (Cat#5741S, 1:1000, CST), anti- β -catenin (Cat#8480S, 1:1000, CST), anti-P- β -catenin (Cat#5741S, 1:1000, CST), anti-GSK-3 β (Cat#5741S, 1:1000, CST), anti-P-GSK-3 β (Cat#5558S, 1:1000, CST), anti-Axin1 (Cat#5863S, 1:1000, CST), anti-APC (Cat#2504S, 1:1000, CST), PCNA (Cat#10205-2-AP, 1:1000, Proteintech) and anti-GAPDH (Cat#5174S, 1:2000, CST) at 4 °C. The next day, after restoration to room temperature, PVDF membrane was incubated with horseradish peroxidase labeled anti-rabbit IgG (Cat#7074S, 1:5000, CST) and anti-mouse IgG (Cat#7076S, 1:5000, CST) correspondingly for 1 h at room temperature. After chemiluminescence and image development, the images were exposed to

a gel imaging system (Bio-RAD, Hercules, CA, USA). Protein expression was normalized to GAPDH.

Immunohistochemistry (IHC) Staining

Paraffin sections were cut into 4 μm thick pieces and mounted on silanized slides. For HCC tissues, after being taken out of the microwave oven at 95 $^{\circ}\text{C}$, the antigen was incubated with ARHGAP17 primary antibody (Cat#ab74454, 1:200, Abcam) for 10 min, and secondary antibody for 1 h at room temperature, successively. Next the sections were incubated with diaminobenzidine (DAB). The images were obtained by re-staining with hematoxylin. IHC analysis was performed by two independent investigators simultaneously. The positive expression intensity of IHC is reflected by the integrated optical density (IOD), specifically the IOD sum/Area sum.

Immunofluorescence (IF)

The prepared paraffin sections of HCC tissues were dewaxed to water. After the antigen repair in a microwave oven, 3% BSA was added for 30 min of incubation at room temperature, followed by an incubation with ARHGAP17 antibody overnight at 4 $^{\circ}\text{C}$ and secondary antibody at room temperature in a dark place for 50 min, successively. The nuclei were re-stained with DAPI. Image acquisition was conducted under a fluorescence microscope.

Statistical Analysis

Data were expressed as mean \pm standard deviation (SD). GraphPad Prism 6 software was used for statistical analysis. A difference between the two groups was performed by Student's *t* test, and a difference among three or more groups was compared by one-way analysis of variance (ANOVA) followed by Tukey's post hoc test. If $p < 0.05$, there was a statistical significance.

Results

ARHGAP17 Expression in HCC Tissues and Cells

The expression of ARHGAP17 was detected in 12 cases of human HCC tissues and 11 cases of para-cancer tissues by IHC staining, which demonstrated that ARHGAP17 was mainly expressed in the cytoplasm of cancer cells, and ARHGAP17 staining in HCC tissues was significantly lowered as compared with para-cancer tissues (Fig. 1A). The IF intensity of ARHGAP17 in HCC tissue is also lower than that of para-cancer tissues (Fig. 1B).

HCC cells were induced by TGF- β 1 to undergo EMT, after which, an interstitial change in the morphology of Bel-7405 occurred, while Huh7 showed no significant

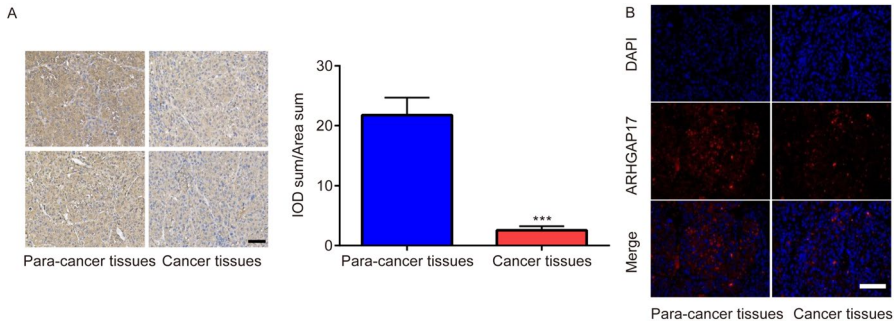


Fig. 1 Decreased ARHGAP17 expression in HCC tissues. IHC staining was used to detect ARHGAP17 expression in HCC tissues and para-cancer tissues (A). IF was used to detect ARHGAP17 expression in HCC tissues and para-cancer tissues (B). Scar bar, 100 μ m. *** $P < 0.001$, vs. para-cancer tissues, $n = 3$

morphological change (Fig. 2A); Meanwhile, the mRNA (Fig. 2B and C) and protein (Fig. 2D–F) expressions of ARHGAP17 and epithelial marker E-cadherin decreased significantly, while the mRNA (Fig. 2B and C) and protein (Fig. 2D–F) expressions of mesenchymal marker N-cadherin increased significantly in TGF- β group in comparison with ctrl group.

Overexpression of ARHGAP17 Inhibits the Proliferation and Invasion of HCC Cells In Vitro

To investigate the influence of ARHGAP17 on the progression of HCC, Bel-7405 and Huh7 cells were transduced with lentivirus, afterwards, cell proliferation, migration, and invasion were analyzed. For Bel-7405 and Huh7, mRNA and protein

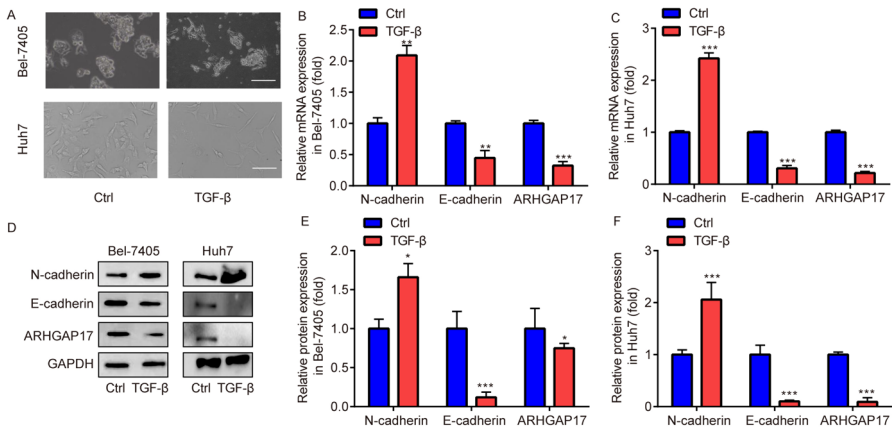


Fig. 2 Downregulated ARHGAP17 expression in TGF- β -induced cells. After Bel-7405 and Huh7 were induced by TGF- β for 3 days, the cell morphologies were observed under an optical microscope (A), mRNA (B and C) and protein (D–F) expressions of E-cadherin, N-cadherin and ARHGAP17 were evaluated by RT-qPCR and western blot. Scar bar, 100 μ m. ** $P < 0.01$, *** $P < 0.001$, versus ctrl, $n = 3$

expressions of ARHGAP17 in lentivirus-transduced cells were significantly higher than empty vector lentivirus-transduced cells or control cells (Fig. 3A and B). In ARHGAP17 lentivirus-transduced Bel-7405 and Huh7, cell proliferation (Fig. 3C and D), and cell invasion (Fig. 3E), were significantly lower compared to that of empty vector group or control group. These findings indicated that the proliferation and invasion capacities of HCC cells were significantly reduced by overexpression of ARHGAP17.

ARHGAP17 Suppressed HCC Growth In Vivo

To investigate the inhibition of tumor growth by ARHGAP17 in vivo, untreated Bel-7405, Bel-7405 with empty vector, and Bel-7405 overexpressing ARHGAP17 were implanted into the right axilla of mice to form ectopic tumors.

From day 27–39, tumor volume in ARHGAP17/Bel-7405 group was significantly smaller than that of empty vector group or control group (Fig. 4A and B). At day 39, tumor weight in ARHGAP17/Bel-7405 group was also significantly lower than that of empty vector group or control group (Fig. 4C). Both the IHC assay and the IF assay showed that the staining intensity and fluorescence intensity of tumors

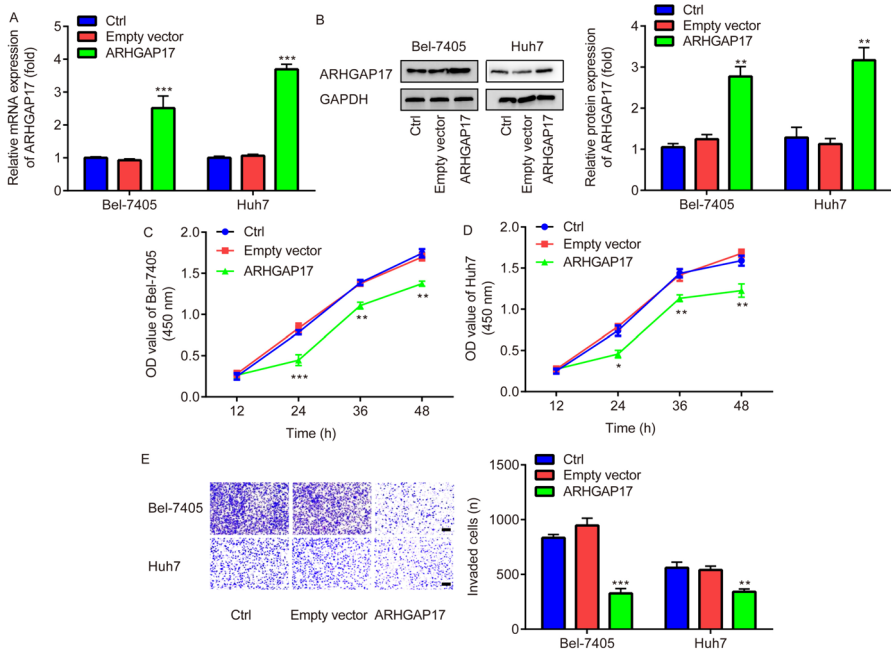


Fig. 3 Overexpression of ARHGAP17 inhibits the HCC cell proliferation and invasion in vitro. Detection of ARHGAP17 expression in Bel-7405 and Huh7 transfected with ARHGAP17 vector and empty vector by RT-qPCR and western blot (A and B). Bel-7405 and Huh7 were subjected to CCK8 assay (C and D), and invasion assay (E). Scar bar, 10 μ m. * P < 0.05, ** P < 0.01, *** P < 0.001, vs. empty vector or ctrl group, n = 3

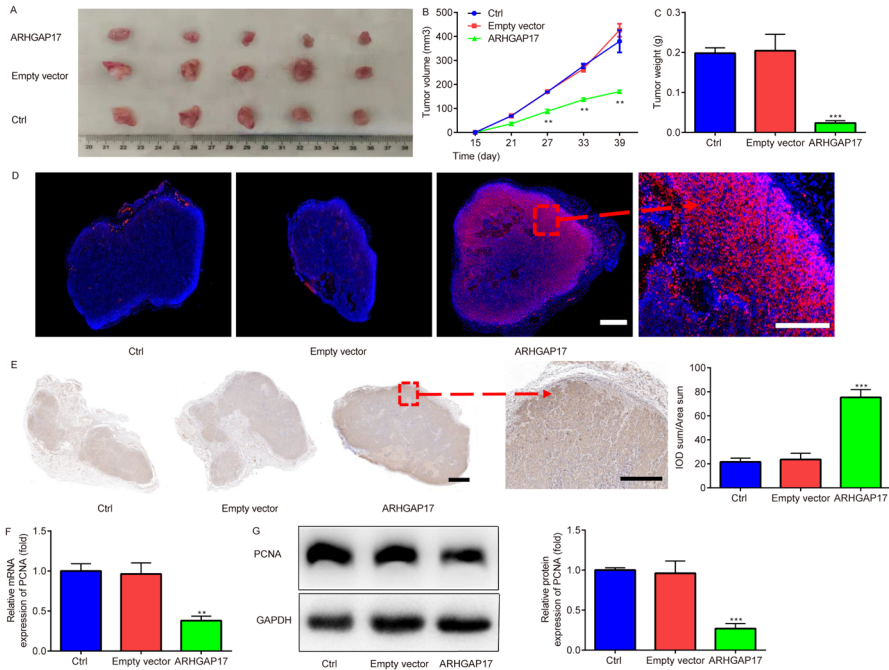


Fig. 4 Overexpression of ARHGAP17 suppressed HCC tumor growth in vivo. Comparison of tumor size (A and B) and tumor weight (C) after subcutaneous implantation of cells in nude mice. ARHGAP17 expression in tumor tissues was detected by IF (D), and IHC (E). mRNA and protein expressions of PCNA were evaluated by RT-qPCR and western blot (F and G). Scar bar, 100 μ m, * P < 0.05, ** P < 0.01, *** P < 0.001, versus empty vector or ctrl group, n = 5

overexpressing ARHGAP17 were significantly higher than those of empty vector group or control group (Fig. 4D and E).

As acknowledged, PCNA expression stands for an index of cell proliferation in various neoplasms (Park et al. 2016). Current study observed that, mRNA and protein expressions of PCNA were significantly higher than those of empty vector group or control group (Fig. 4F and G).

ARHGAP17 was Negatively Associated with Wnt Pathway in HCC

Considering the important role of ARHGAP17 in HCC tumor growth, current study intended to explore its potential molecular mechanism. EMT plays a decisive role in the progression and distant colonization of HCC (Sengez et al. 2022). As acknowledged, activation of Wnt signaling pathway promotes the occurrence of EMT (Yang et al. 2017). It is speculated that EMT and Wnt signaling pathways are related to ARHGAP17, ARHGAP17 inhibits the progression of HCC by inactivation of Wnt signaling pathway.

Consequently, the present study evaluated the role of Wnt signaling pathway in ARHGAP17 overexpressing HCC cells. After ARHGAP17 was overexpressed in

Bel-7405 and Huh7, the changes in mRNA levels of Wnt signaling pathway-related molecules, e.g., β -catenin was decreased, while GSK3 β , APC and AXIN1 were increased (Fig. 5A and B); the changes in protein levels (or ratios) of Wnt signaling pathway-related molecules, e.g., p- β -catenin/ β -catenin ratio, APC, and AXIN1 were increased, while p-GSK3 β /GSK3 β ratio decreased (Fig. 5C–E).

Discussion

Essentially, the RoGAP reaction catalyzes the inherent GTP-enzyme activity of Rho protein (Braun and Olayioye 2015). Though several RhoGAPs have been identified to be tumor suppressors in various cancers (Tripathi et al. 2014; Ravi et al. 2015), little is known about the function of ARHGAP17 in HCC carcinogenesis. Current study demonstrated for the first time that ARHGAP17 expression in HCC was significantly lower than that in paracancerous tissues. ARHGAP17 inhibited cell proliferation, migration, and invasion in vitro and attenuates the tumorigenicity in vivo, which at least partially by inactivating the Wnt/ β -catenin signaling pathway in HCC.

At the beginning, ARHGAP17 expression is down-regulated in HCC, suggesting the tumor suppressive role of ARHGAP17 in HCC. In TGF- β -induced HCC cells, there was a significantly reduced expression of ARHGAP17.

EMT is a multistage process, which leads to the breakdown of intercellular adhesion complex, loss of characteristic features of epithelial cells, and transformation into mesenchymal fibroblast phenotypes (Hao et al. 2019). Increased E-cadherin reduced the ability of cells to invade, as E-cadherin loss is a major

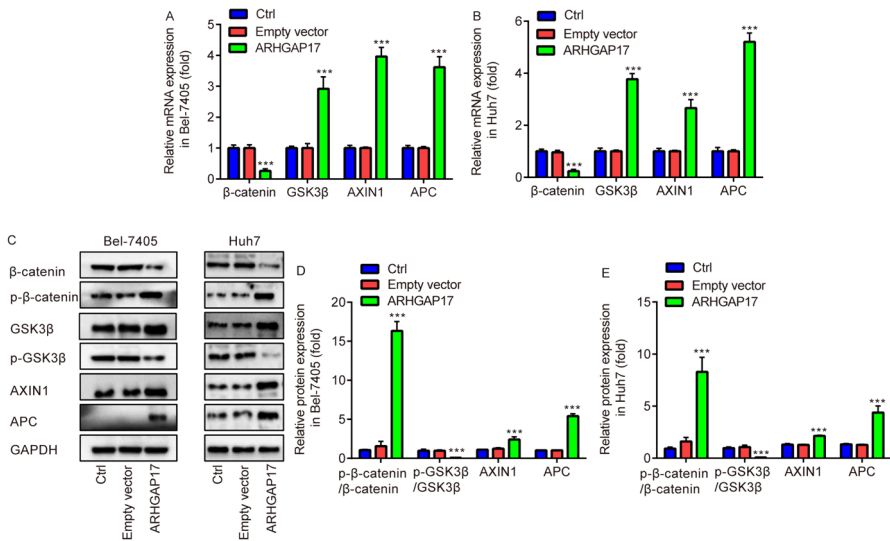


Fig. 5 ARHGAP17 overexpression inactivated the Wnt pathway in HCC. After Bel-7405 and Huh7 were transfected with ARHGAP17 vector, mRNA and protein expressions of Wnt/ β -catenin signaling pathway-related molecules were analyzed by RT-qPCR (A and B), western blot (C–E). ** $P < 0.01$, *** $P < 0.001$, versus empty vector, $n = 3$

feature of EMT (Wong et al. 2018). In numerous cancers, decrease of E-cadherin and increase of N-cadherin are implicated in malignant process and poor patient outcomes. The mechanisms include enhanced tumor cell invasion, lymph node and foreign metastases facilitated by a process named epithelial to EMT (Gumbiner 2005). E-cadherin endocytosis leads to the release of β -catenin and promotes the expression/transcription of Snail-1 by Wnt/ β -catenin signaling pathway (Gomaa et al. 2021). After EMT, tumor cells acquire an interstitial phenotype in HCC, which greatly increases the potential for invasion, resulting in HCC cells colonizing distant organs (Wang et al. 2020a, b). Based on the decreased expression of ARHGAP17 after EMT, current study speculated that ARHGAP17 might play a key role in the distant colonization of HCC.

Thereafter, the proliferation and invasion capacities of HCC cells with overexpression of ARHGAP17 were significantly reduced; in addition, *in vivo* tumor transplantation experiments also verified the inhibitory effect of ARHGAP17 in HCC. However, the underlying molecules of the function of ARHGAP17 in HCC have not been discovered.

EMT is dependent on the coordinated activity of a number of signal transduction pathways, including TGF- β , MAPK, PI3K/Akt, and Wnt/ β -catenin signaling pathways, all of which play important roles (Zhang et al. 2019; Klauzinska et al. 2020; Zhang and Wang 2020). As acknowledged, ARHGAP17 is negatively correlated with β -catenin gene (CTNNB1) (Jiang et al. 2018), phosphorylation of Gsk3 β on Ser9 residues inactivates Gsk3 β , promoting the activation of β -catenin (Kim et al. 2021). Herein, ARHGAP17 overexpression was found to significantly induce p-GSK3 β and reduced p- β -catenin expression, indicating the inactivation of Wnt pathway.

In summary, ARHGAP17 inhibits cell proliferation and invasion by Wnt/ β -catenin signaling pathway.

Author Contributions HZ, SF, and WZ conceived and designed the experiments. CL, MS, FC analyzed the data. CL, YZ, BN, HZ performed the experiments. The manuscript was written by HZ, SF, and WZ. All authors read and approved the final manuscript.

Funding This work was supported by the Natural Science Foundation of Liaoning Province (2019-ZD-1062), the Joint Program of Key R&D Programs of Liaoning Province (2020JH2/10300168), Medical and Industrial Cross Joint Project of Liaoning Province (2022-YGJC-11) and the R&D Project for Major Technological Innovations of Shenyang City (19-112-4-081).

Data Availability All data generated or analyzed during this study are included in this published article.

Declarations

Competing interests The author reports no conflicts of interest in this work.

Ethical Approval Current study was approved by the Ethics Committee of the General Hospital of Northern Theater Command of PLA.

Informed Consent Written informed consent was obtained from the parents.

Consent for Publication The authors affirm that human research participants provided informed consent for publication of the images.

References

- Braun AC, Olayioye MA (2015) Rho regulation: Dlc proteins in space and time. *Cell Signal* 27:1643–1651
- Forner A, Reig M, Bruix J (2018) Hepatocellular carcinoma. *Lancet* 391:1301–1314
- Ghouri YA, Mian I, Rowe JH (2017) Review of hepatocellular carcinoma: epidemiology, etiology, and carcinogenesis. *J Carcinog* 16:1
- Gomaa W, Al-Maghrabi H, Al-Maghrabi J (2021) The prognostic significance of immunostaining of Wnt signalling pathway molecules, E-cadherin and β -catenin in colorectal carcinomacolorectal carcinoma. *Arab J Gastroenterol* 22:137–145
- Gumbiner BM (2005) Regulation of cadherin-mediated adhesion in morphogenesis. *Nat Rev Mol Cell Biol* 6:622–634
- Guo Q, Xiong Y, Song Y, Hua K, Gao S (2019) ARHGAP17 suppresses tumor progression and up-regulates P21 and P27 expression via inhibiting PI3K/AKT signaling pathway in cervical cancer. *Gene* 692:9–16
- Hao Y, Baker D, Ten Dijke P (2019) TGF- β -mediated epithelial-mesenchymal transition and cancer metastasis. *Int J Mol Sci* 20:2767
- Jaffe AB, Hall A (2005) Rho gtpases: biochemistry and biology. *Annu Rev Cell Dev Biol* 21:247–269
- Jiang W, He T, Liu S, Zheng Y, Xiang L, Pei X, Wang Z, Yang H (2018) The PIK3CA E542K and E545K mutations promote glycolysis and proliferation via induction of the β -catenin/SIRT3 signaling pathway in cervical cancer. *J Hematol Oncol* 11:139
- Kim JG, Mahmud S, Min JK, Lee YB, Kim H, Kang DC, Park HS, Seong J, Park JB (2021) RhoA GTPase phosphorylated at tyrosine 42 by src kinase binds to β -catenin and contributes transcriptional regulation of vimentin upon Wnt3A. *Redox Biol* 40:101842
- Klauzinska M, Castro NP, Rangel MC, Spike BT, Gray PC, Bertolette D, Cuttitta F, Salomon D (2020) The multifaceted role of the embryonic gene *Cripto-1* in cancer, stem cells and epithelial-mesenchymal transition. *Semin Cancer Biol* 29:51–58
- Kreider-Letterman G, Castillo A, Mahlandt EK, Goedhart J, Rabino A, Goicoechea S, Garcia-Mata R (2023) ARHGAP17 regulates the spatiotemporal activity of Cdc42 at invadopodia. *J Cell Biol* 222:e202207020
- Malfettone A, Soukupova J, Bertran E et al (2017) Transforming growth factor- β -induced plasticity causes a migratory stemness phenotype in hepatocellular carcinoma. *Cancer Lett* 392:39–50
- McGlynn KA, Petrick JL, El-Serag HB (2021) Epidemiology of hepatocellular carcinoma. *Hepatology* 73:4–13
- Pan S, Deng Y, Fu J, Zhang Y, Zhang Z, Ru X, Qin X (2018) Tumor suppressive role of ARHGAP17 in colon cancer through Wnt/ β -Catenin signaling. *Cell Physiol Biochem* 46:2138–2148
- Park SY, Jeong MS, Han CW, Yu HS, Jang SB (2016) Structural and functional insight into proliferating cell nuclear antigen. *J Microbiol Biotechnol* 26:637–647
- Rabaan AA, Al-Ahmed SH, Bazzi AM, Alfouzan WA, Alsuliman SA, Aldrazi FA, Haque S (2020) Overview of hepatitis C infection, molecular biology, and new treatment. *J Infect Public Health* 13:773–783
- Ravi A, Kaushik S, Ravichandran A, Pan CQ, Low BC (2015) Epidermal growth factor activates the rho gtpase-activating protein (gap) deleted in liver cancer 1 via focal adhesion kinase and protein phosphatase 2a. *J Biol Chem* 290:4149–4162
- Richnau N, Aspenström P (2001) Rich, a rho GTPase-activating protein domain-containing protein involved in signaling by Cdc42 and Rac1. *J Biol Chem* 27:35060–35070
- Sengez B, Carr BI, Alotaibi H (2022) EMT and inflammation: crossroads in HCC. *J Gastrointest Cancer*. <https://doi.org/10.1007/s12029-021-00801-z>
- Shao S, Zhao X, Zhang X, Luo M, Zuo X, Huang S, Wang Y, Gu S, Zhao X (2015) Notch1 signaling regulates the epithelial-mesenchymal transition and invasion of breast cancer in a Slug-dependent manner. *Mol Cancer* 14:28

- Sribenja S, Sawanyawisuth K, Kraiklang R, Wongkham C, Vaeteewoottacharn K, Obchoei S, Yao Q, Wongkham S, Chen C (2013) Suppression of thymosin β 10 increases cell migration and metastasis of cholangiocarcinoma. *BMC Cancer* 13:430
- Tian Q, Gao H, Zhou Y, Zhu L, Yang J, Wang B, Liu P, Yang J (2022) RICH1 inhibits breast cancer stem cell traits through activating kinases cascade of Hippo signaling by competing with Merlin for binding to Amot-p80. *Cell Death Dis* 13:71
- Tripathi BK, Qian X, Mertins P, Wang D, Papageorge AG, Carr SA, Lowy DR (2014) Cdk5 is a major regulator of the tumor suppressor dlc1. *J Cell Biol* 207:627–642
- Wang J, He H, Jiang Q, Wang Y, Jia S (2020a) CBX6 promotes HCC metastasis via transcription factors Snail/Zeb1-mediated EMT mechanism. *Onco Targets Ther* 13:12489–12500
- Wang L, Yang X, Wan L, Wang S, Pan J, Liu Y (2020b) ARHGAP17 inhibits pathological cyclic strain-induced apoptosis in human periodontal ligament fibroblasts via Rac1/Cdc42. *Clin Exp Pharmacol Physiol* 47:1591–1599
- Wong SHM, Fang CM, Chuah LH, Leong CO, Ngai SC (2018) E-cadherin: its dysregulation in carcinogenesis and clinical implications. *Crit Rev Oncol Hematol* 121:11–22
- Yang S, Liu Y, Li MY et al (2017) FDX3 promotes tumor growth and metastasis by activating Wnt/ β -catenin signaling pathway and EMT in non-small cell lung cancer. *Mol Cancer* 16:124
- Zhang Y, Wang X (2020) Targeting the Wnt/ β -catenin signaling pathway in cancer. *J Hematol Oncol* 13:165
- Zhang J, Wang J, Zhou YF, Ren XY, Lin MM, Zhang QQ, Wang YH, Li X (2015) Rich1 negatively regulates the epithelial cell cycle, proliferation and adhesion by CDC42/RAC1-PAK1-Erk1/2 pathway. *Cell Signal* 27:1703–1712
- Zhang Y, Li S, Zhou X, Sun J, Fan X, Guan Z, Zhang L, Yang Z (2019) Construction of a targeting nanoparticle of 3',3"-bis-peptide-siRNA conjugate/mixed lipid with postinserted DSPE-PEG2000-cRGD. *Mol Pharm* 16:4920–4928

Publisher's Note Springer Nature remains neutral with regard to jurisdictional claims in published maps and institutional affiliations.

Springer Nature or its licensor (e.g. a society or other partner) holds exclusive rights to this article under a publishing agreement with the author(s) or other rightsholder(s); author self-archiving of the accepted manuscript version of this article is solely governed by the terms of such publishing agreement and applicable law.